catalysts

MDPI

Article

Microcystis aeruginosa Synergistically Facilitate the Photocatalytic Degradation of Tetracycline Hydrochloride and Cr(VI) on PAN/TiO_2/Ag Nanofiber Mats

Lei Wang [1], Changbo Zhang [2,*], Rong Cheng [3,*], Jafar Ali [1,4], Zhenbo Wang [5,6,*], Gilles Mailhot [7] and Gang Pan [1,8,*]

1 Key Laboratory of Environmental Nanotechnology and Health Effects, Research Center for Eco-Environmental Sciences, Chinese Academy of Sciences, 18 Shuangqing Road, Beijing 100085, China; leiwang@rcees.ac.cn (L.W.); jafar_386@yahoo.com (J.A.)
2 Agro-Environmental Protection Institute, Ministry of Agriculture, Tianjin 300191, China
3 School of Environment and Natural Resources, Renmin University of China, Beijing 100872, China
4 Research Center for Environmental Material and Pollution Control Technology, University of Chinese Academy of Sciences, Beijing 100049, China
5 Institute of Geographic Sciences and Natural Resources Research, Chinese Academy of Sciences, 11A Datun Road Chaoyang District, Beijing 100101, China
6 Key Laboratory of Regional Sustainable Development Modeling, Chinese Academy of Sciences, Beijing 100101, China
7 CNRS, SIGMA Clermont, Institut de Chimie de Clermont-Ferrand, Université Clermont Auvergne, F-63000 Clermont-Ferrand, France; gilles.mailhot@uca.fr
8 Center of Integrated Water-Energy-Food Studies (iWEF), School of Animal, Rural, and Environmental Sciences, Nottingham Trent University, Brackenhurst Campus, NG25 0QF, UK
* Correspondence: zhchb1976@163.com (C.Z.); chengrong@ruc.edu.cn (R.C.); wangzb@igsnrr.ac.cn (Z.W.); gpan@rcees.ac.cn (G.P.); Tel.: +86-10-6294-3436 (G.P.)

Received: 24 October 2018; Accepted: 29 November 2018; Published: 5 December 2018

Abstract: Cyanobacterial blooms can cause serious damage to aquatic ecosystems. However, we have demonstrated that typical algae-blooming species *Microcystis aeruginosa (M. aeruginosa)* combined with photocatalysts could synergistically facilitate the photodecontamination of tetracycline hydrochloride (TC) and Cr(VI). In this study, for the first time, harmful algae were successfully converted into photoreactive bionano hybrid materials by immobilizing *M. aeruginosa* cells onto polyacrylonitrile (PAN)-TiO_2/Ag hybrid nanofibers, and their photocatalytic activity was evaluated. The addition of *M. aeruginosa* significantly improved the photodecontamination, and the reaction rate constant (k) values of TC and Cr(VI) degradation by *M. aeruginosa*-PAN/TiO_2/Ag nanofiber mats were 2.4 and 1.5-fold higher than that of bare PAN/TiO_2/Ag nanofiber. Photoreaction caused damage to algae cells, but no microcystin was found that had been photodegraded simultaneously. The effects of various active species were also investigated, and the photodegradation mechanism was proposed. Recycling tests revealed that this flexible *M. aeruginosa*-PAN/TiO_2/Ag hybrid mat had potential application in the removal of mixed organic and inorganic pollutants with high efficiency and without secondary pollutants. Thus, harmful algae blooms could serve as an efficient materials to remove toxic pollutants in a sustainable way under visible light irradiation.

Keywords: *Microcystis aeruginosa*; PAN nanofiber; TiO_2 photocatalytic; Ag nanoparticles; tetracycline; Cr(VI)

1. Introduction

Microalgae are one of the most important bio resources and are distributed widely within various aquatic ecosystems. Microalgae remediation of environmental pollutants has attracted scientific attention, as micro algal remediation is **a** cost-effective, solar power-driven, and sustainable reclamation strategy [1]. Some studies have demonstrated that algae species such as, *Chlorella vulgaris, Chlamydomonas sajao, Nitzschia hantzschiana,* and *Anabaena cylindrical* can induce the photo-decontamination of pollutants under irradiation [2–5]. During photochemical reactions, algae cells release organic acids and chlorophyll, which can absorb photons and induce the generation of active radicals [6]. When algae are combined with other photochemically active substances such as ferric ions, the system presents improved photocatalytic activity [7]. *M. aeruginosa* is a typical species in cyanobacterial blooms and has been found widely in lakes in China [8,9]. Current studies concerning *M. aeruginosa* mainly focus on its inactivation and removal because of its extensive damage to aquatic ecosystems. However, little is known regarding the photochemical activity of *M. aeruginosa* and its combination with other nanomaterials to prepare photoreactive biocomposite materials. The role of *M. aeruginosa* in the simultaneous phototransformation of organic and inorganic pollutants has not been reported yet.

There are some drawbacks associated with the use of the algae-suspension photoreaction system during the recovery of algae cells. The immobilization of algae cells can help to remove cells from the photoreaction system. Nanofiber mats present a decent matrix to load algae cells because of high pore volume, large specific surface area, and uniform microporosity [10]. Electrospun polymer nanofibers with Ag/TiO_2 nanoparticles have attracted much attention recently, due to their enhanced characteristics, such as their antimicrobial, optical, and photocatalytic properties [11–14]. However, most of the published studies have opted for two-step methods to decorate Ag/TiO_2 nanoparticles on nanofibers, which are more complicated and less efficient [15]. Polyacrylonitrile (PAN)-based hybrid nanofibers are water insoluble and can be easily recovered from solution. Moreover, they have highly specific surface areas and functional nanoparticles; thus, these merits enhance their potential application [16,17]. In this work, we used a one-step method to prepare PAN/TiO_2/Ag nanofibers (PAN/TiO_2/Ag NF), and solvents such as N,N-dimethylformamide (DMF) served as electrospinning reducing agents for the synthesis of metallic Ag nanoparticles (AgNPs) [18]. Until now, very few studies have been reported regarding decorating PAN-based hybrid nanofiber mats with microalgae. This novel bionano hybrid material may presents integrated properties of nanomaterials and microorganisms, which would be worth investigating further. Moreover, there is still a lack of knowledge concerning the synergistic photocatalytic activity of *M. aeruginosa* and PAN/TiO_2/Ag hybrid nanomaterials.

Therefore, the objective of this work was to prepare photo reactive bionano hybrid materials by immobilizing *M. aeruginosa* cells onto PAN/TiO_2/Ag nanofiber mats and study their synergistic photocatalytic degradation of organic and inorganic pollutants under visible light irradiation. This is the first time that harmful algae *M. aeruginosa* have been utilized to photodegrade mixed pollutants under visible light irradiation. This study can help to explain one of the possible transformation pathways of pollutants in the aquatic ecosystem. Antibiotics and heavy metals are two major classes of highly concerned environmental pollutants, hence tetracycline hydrochloride (TC) and Cr(VI) were selected as target pollutants in this work [19–23]. The effects of various active species on the decontamination of pollutants were also investigated. Microcystins were analyzed at the end of the reaction, and the stability of photo-reactive bionano hybrid materials was also validated by recycling tests.

2. Results and Discussion

2.1. Characterization of M. aeruginosa-Decorated PAN/TiO_2/Ag Nanofiber Mats

Figure 1 shows the scanning electron microscope (SEM) images of PAN-based nanofibers comprising 2 wt% of TiO_2 and 5 wt% of $AgNO_3$. PAN/TiO_2 nanofiber appeared to have a rough and non-uniform morphology with diameters above 270 nm, however the PAN/Ag nanofibers displayed

a smooth morphology with an average diameter of 130 nm. Interestingly, the spinning potential of the mixture was enhanced by $AgNO_3$ and formed uniform PAN/TiO_2/Ag functional nanofibers with a diameter of 200 nm and specific surface area of 49 m^2 g^{-1}. Figure 2(a2–c2) depicts the EDX spectra of these nanofiber mats. The characteristic peaks of Ag and Ti provided further evidence for the synthesis of AgNPs and TiO_2 on surface of nanofibers.

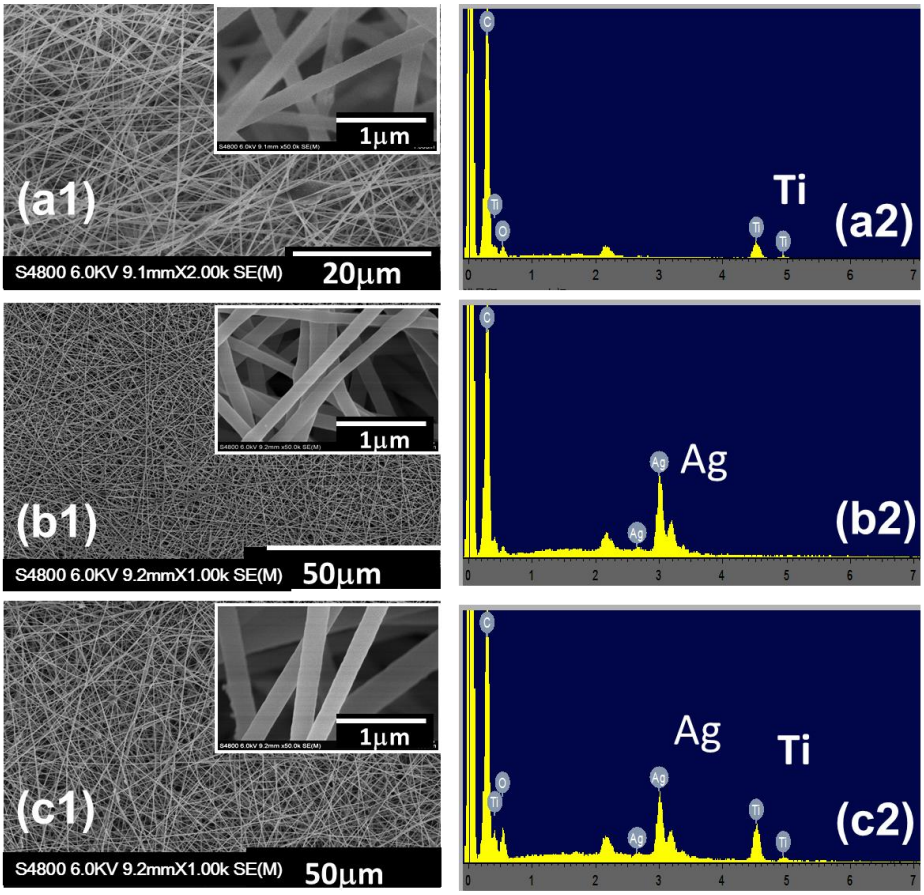

Figure 1. Scanning electron microscopy (SEM) images and energy-dispersive x-ray spectroscopy of various hybrid nanofiber mats: (**a1**, **a2**) PAN/2%TiO_2, (**b1**, **b2**) PAN/5%$AgNO_3$, and (**c1**, **c2**) PAN/2%TiO_2/5% $AgNO_3$.

The transmission electron microscopy (TEM) images show the well-dispersed Ag and TiO_2 nanoparticles on the nanofibers (Figure 2a). The crystal-phase structure of PAN/TiO_2/Ag hybrid materials were also measured using X-ray diffraction (XRD) measurements. Figure 2b shows the XRD pattern of the PAN/TiO_2/Ag NF, which exhibits the characteristic (101), (200), (105), (211), and (204) reflections corresponding to the lattice planes of anatase TiO_2. The peaks appeared at the 2θ of 38.4 and 44.2, which were attributed to the diffraction peaks of AgNPs (111) and (200). The UV–vis spectra of the ultrathin hybrid nanofiber mats were also characterized. As shown in Figure 3c, the PAN/Ag and PAN/TiO_2/Ag NF displayed higher visible absorption than PAN and PAN/TiO_2 NF. This absorptive characteristic is mainly ascribed to a major role played by AgNPs in decreasing the band gap of TiO_2. These findings also corroborate our previous studies [24–26].

M. aeruginosa decorated nanofiber mats were obtained by placing the algae solution on the surface of PAN/TiO_2/Ag NF and then keeping them in an incubator for 72 h to allow for the adequate attachment of the microalgae on the surface of the nanofibers. The unstable cells were removed, and there was no more release of algae into the solution, even after 8 washes (Figure S1). These nanofibers with highly specific surface areas present a good matrix for algae cell immobilization. The detailed morphology of this bionano hybrid material was further analyzed by SEM, which revealed that the microalgae had been well immobilized on the nanofibers (Figure 3). In order to study the interaction

between algae and PAN/TiO_2/Ag NF, the UV-vis analysis of algae-modified PAN/TiO_2/Ag NF was performed. Figure 2c shows a certain shift toward visible region, with highly intense absorption curves around the entire visible region, but a small decrease in the UV region ($\lambda < 300$ nm). This can be attributed to the formation of a complex between algae-released substances and TiO_2 nanoparticles.

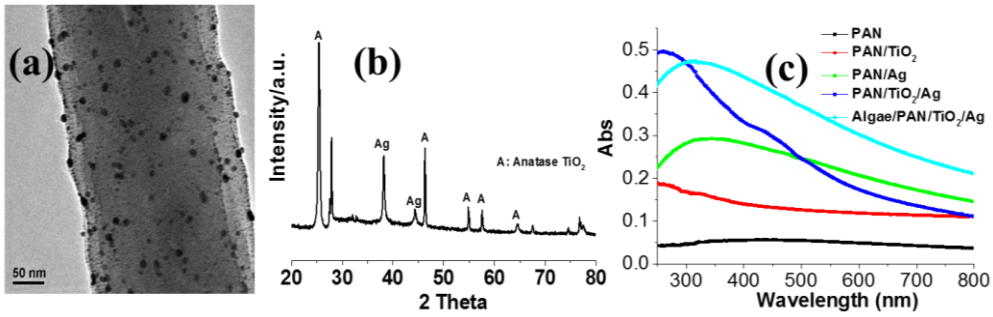

Figure 2. (**a**) Transmission electron microscopy (TEM) image and (**b**) X-ray diffraction (XRD) pattern of PAN/TiO_2/Ag hybrid nanofiber; (**c**) UV-vis spectra of PAN hybrid nanofibers.

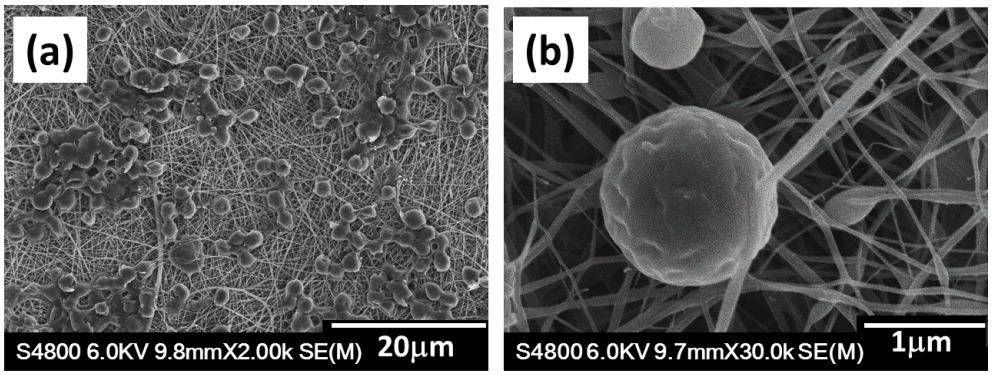

Figure 3. SEM images of *M. aeruginosa* on the surface of PAN/TiO_2/Ag hybrid nanofiber mats at (**a**) low and (**b**) high magnification.

2.2. Photocatalytic Decontamination of TC and Cr(VI)

The photocatalytic activities of *M. aeruginosa*-PAN/TiO_2/Ag bionano hybrid mats were evaluated by simultaneous removal of TC and Cr(VI) under visible light irradiation ($\lambda > 420$ nm) and ambient conditions. Systems with only *M. aeruginosa* (1.0×10^7 cells L^{-1}) or PAN/TiO_2/Ag NF (1 g L^{-1}) were set as controls. In the control systems, the number of algae cells were equal to the nanofiber mat, and the amount of PAN/TiO_2/Ag NF was the same as that used for algae immobilization. Before irradiation, TC and Cr(VI) mixed solutions with *M. aeruginosa*, PAN/TiO_2/Ag NF, or *M. aeruginosa*-PAN/TiO_2/Ag NF were separately stirred in dark ambient conditions for 30 min to achieve the adsorption–desorption equilibrium. The *M. aeruginosa*-PAN/TiO_2/Ag NF absorbed 13% of TC and 11% of Cr(VI) in 30 min, which was higher than that of only *M. aeruginosa* or PAN/TiO_2/Ag NF (as shown in Figure 4a,b). Extracellular substances of algae such as lipids and polysaccharides deliver various organic functional groups to sequester metal ions or organic pollutants[6]. Fresh algae cells combined with nanofibers can improve the bonding of mixed pollutants on nanofiber mats, which is important for enhanced photodegradation process. The irradiation results demonstrated that *M. aeruginosa*-PAN/TiO_2/Ag NF exhibited efficient activities for simultaneous TC degradation and Cr(VI) reduction. The photoremoval rates of TC and Cr(VI) reached up to 96% and 75%, respectively. However, only 77% and 41% of the TC, and 61% and 34% of the Cr(VI), could be removed within the same reaction time using pure PAN/TiO_2/Ag NF and *M. aeruginosa*, respectively. The addition of *M. aeruginosa* apparently enhanced the photocatalytic activity of the PAN/TiO_2/Ag. The variation of the UV–vis

absorption spectra of algae supernatant was studied. The absorbance of irradiated algae supernatant was much higher than that of the living algae supernatant, which was attributed to the fact that algae exposed to irradiation released many substances (such as pigments, carboxylic acids) into the aqueous solution (Figure S2). Thus, the underlying mechanism behind the enhanced photodegradation of target pollutants can be explained, as algae that release intracellular substances (organic acids and chlorophylls) can consume holes and cause effective separation of photogenerated electron-holes on TiO_2 and facilitate the photocatalytic activity of PAN/TiO_2/Ag NF. For the first time, this work tested the photodegradation of TC and Cr(VI) induced by only *M. aeruginosa* cells and confirmed its efficiency for the photo-removal of pollutants. This work presents a possible method to turn widespread and harmful algae species into useful photoreactive biomaterials. Current findings can help to explain the possible transformation pathways of pollutant in natural water system.

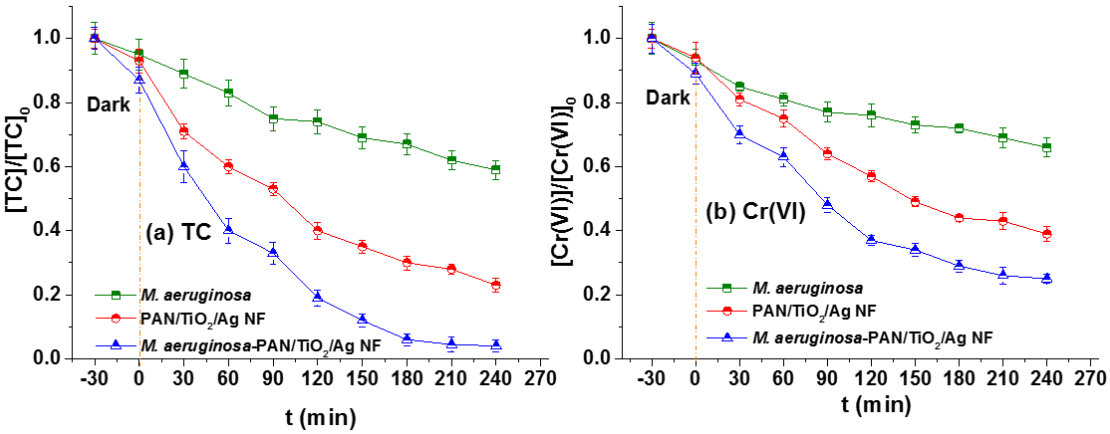

Figure 4. The simultaneous (**a**) degradation of tetracycline hydrochloride (TC) and (**b**) reduction of Cr(VI) under visible light irradiation in various system.

The kinetics analysis is shown in Table 1. TC and Cr(VI) removal fit very well with the pseudo-first order correlation, and *M. aeruginosa*-PAN/TiO_2/Ag NF exhibited the maximum *k* value, according to its high photocatalytic activity. The *k* value for TC degradation by *M. aeruginosa*-PAN/TiO_2/Ag NF was 2.4 fold higher than that of PAN/TiO_2/Ag NF. Also, the *k* value for Cr(VI) removal by *M. aeruginosa*-PAN/TiO_2/Ag NF was 1.5 fold higher than that of PAN/TiO_2/Ag NF. Thus, photocatalytic degradation of TC and Cr(VI) was significantly increased with the addition of *M. aeruginosa*.

Table 1. Kinetics analysis of the photodegradation of TC and Cr(VI).

	Reaction System	K (× 10^{-3}, min^{-1})	Correlation Coefficient R^2
TC	*M. aeruginosa*	1.96 ± 0.15	0.99
	PAN/TiO_2/Ag NF	5.62 ± 0.36	0.99
	M. aeruginosa-PAN/TiO_2/Ag NF	13.21 ± 0.51	0.98
Cr(VI)	*M. aeruginosa*	1.41 ± 0.12	0.94
	PAN/TiO_2/Ag NF	3.72 ± 0.24	0.99
	M. aeruginosa-PAN/TiO_2/Ag NF	5.58 ± 0.38	0.97

k (min^{-1}): reaction rate constant.

2.3. Photodegradation of Algae

Malondialdehyde (MDA) content and superoxide dismutase (SOD) activity in the *M. aeruginosa* were detected after a 4 h reaction. It is evident from Figure 5A that SOD activity was decreased apparently in the system with PAN/TiO_2/Ag NF. Meanwhile, the MDA content in the cells was apparently increased after the reaction (Figure 6B). The MDA content of *M. aeruginosa* in the reaction system with PAN/TiO_2/Ag NF was more than two times higher than without the nanofibers, which

indicates that photocatalytic activity of the PAN/TiO_2/Ag NF may result in lipid peroxidation and cause oxidative stress in *M. aeruginosa*. After irradiation treatment, morphology of the algae was observed by SEM. As shown in Figure 6, *M. aeruginosa* was still immobilized on the nanofibers, however, the cell walls of *M. aeruginosa* were partially damaged, resulting in cell adhesion, holes, and shrinkages. Since the damaged *M. aeruginosa* cells might release microcystins into the system, microcystins were also measured in this work. However, microcystins were not found in the solution after the 4 h reaction. These important findings can also be attributed to the effective photocatalytic activity of PAN/TiO_2/Ag NF, which could simultaneously degrade microcystin in the system.

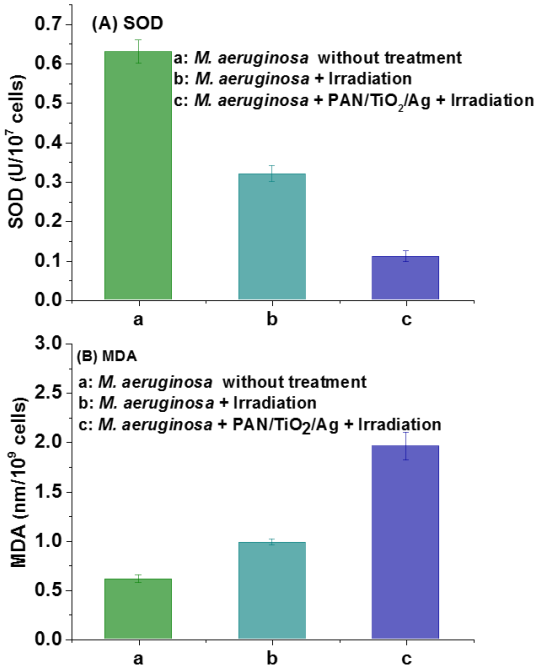

Figure 5. The superoxide dismutase (SOD) activity (**A**) and (**B**) malondialdehyde (MDA) content of algae in different systems.

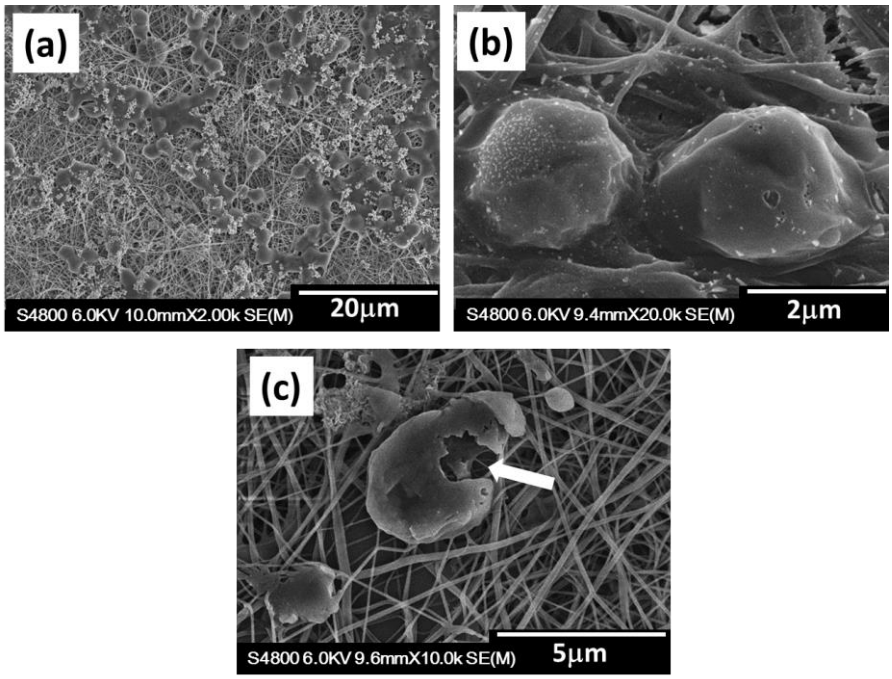

Figure 6. SEM images of photo-damaged algae cells on the surface of PAN/TiO_2/Ag NF at (**a**) low and (**b**, **c**) high magnification.

2.4. Analysis of the Active Species and Discussion of the Mechanism

To explore the underlying mechanism involved in photocatalytic degradation of TC and Cr(VI) by *M. aeruginosa*-PAN/TiO_2/Ag NF, the influences of different active species were studied. Various individual scavengers were applied in the active species trapping experiments to evaluate the effect of the corresponding species, such as KI (hole scavenger), 2-propanol (·OH scavenger), BQ ($O_2^{\cdot-}$ scavenger), and CCl_4 (electron scavenger). Figure 7a reveals that, when KI or 2-propanol was added to the system, the *k* value of TC degradation was much lower than that without radical scavengers, indicating that photogenerated holes and ·OH played important role in the photodegradation of TC. When BQ was added to the reaction system, the reaction was also slightly inhibited, which indicates that $O_2^{\cdot-}$ also took part in the TC degradation. Figure 7b illustrates that, when BQ or CCl_4 were used, the photodegradation of Cr(VI) was significantly inhibited compared with the system without radical scavenger. Therefore, it can be inferred that electrons and $O_2^{\cdot-}$ are active species participating in the reduction of Cr(VI).

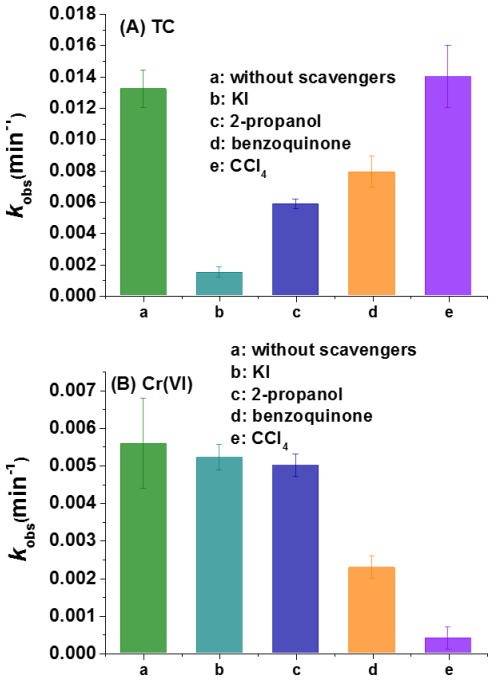

Figure 7. The active species trapping experiments for degradation of TC (**A**) and Cr(VI) (**B**).

A proposed mechanism of removing TC and Cr(VI) using *M. aeruginosa*-PAN/TiO_2/Ag NF is presented in Figure 8. It is well-known that AgNPs can improve the interfacial charge transfer and electron-hole pair separation, thus extending the working area of TiO_2 to visible light region (Figure 3c) [27]. TiO_2/Ag hybrid nanofiber displayed the highest photocatalytic activity under visible light irradiation and contributed by generating the active species (OH, H_2O_2, O_2^-) in the catalysis system [28]. The addition of algae significantly enhanced the photocatalytic performance of PAN/TiO_2/Ag NF. In this bionano hybrid system, the photolysis of algae was enhanced in the presence of PAN/TiO_2/Ag nanofibers, which can help improve the photo-activity of algae cells. Meanwhile, the released algae intracellular organic substances (chlorophylls, humic and fulvic acids, etc.) can consume part of the holes, attenuate electron–hole pair recombination on the TiO_2, and facilitate the photocatalytic activity of PAN/TiO_2/Ag NF [7,29]. The interaction between algae and PAN/TiO_2/Ag NF has been analyzed by the UV-vis spectrum, and Figure 2c shows the formation of a complex between algae-released substances and TiO_2 nanoparticles. Algae cells can improve the absorption ability of toxic pollutants due to their extracellular organic substances release and increase the

number of the functional groups to sequester additional metal ions. They are also able to significantly accelerate the photodegradation of pollutants, because algae intracellular substances (such as chlorophylls) can absorb light energy and generate reactive species (OH, $^1O_2$, HOO, O_2^-) [30,31]. This work demonstrates that pure *M. aeruginosa* can induce the simultaneous photodegradation of TC and Cr(VI) (Figure 4), which is consistent with the previous theory that algae photolysis is a possible strategy for pollutant degradation [32].

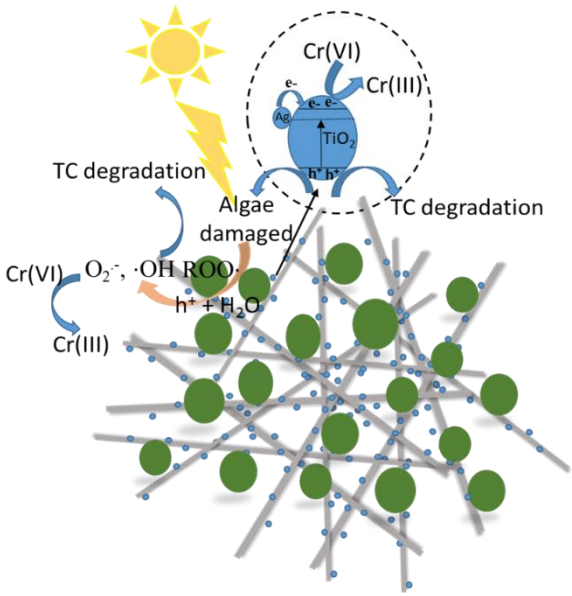

Figure 8. Photocatalytic degradation schematic illustration of TC and Cr(VI) over *M. aeruginosa*-PAN/TiO_2/Ag NF.

2.5. Repeated Test

The reusability and stability of the hybrid nanomaterials were also tested in three cycles. As shown in Figure 9, the removal rate of TC in each cycle was 96%, 90%, and 87%, respectively. Similarly, the removal efficiency of Cr(VI) was also decreased from 75% to 70% after three cycles. Although both slight decrements were observed in each cycle, the *M. aeruginosa*-PAN/TiO_2/Ag NF sustained high activity even after three consecutive cycles and 12 h of continuous irradiation. This result is consistent with the previous results showing that the damaged algae was efficient in the photolysis of pollutants [30,32]. These results demonstrate that bionano hybrid nanofibers have relatively high photocatalytic activity and may be recovered and reused in the combined pollutant treatment.

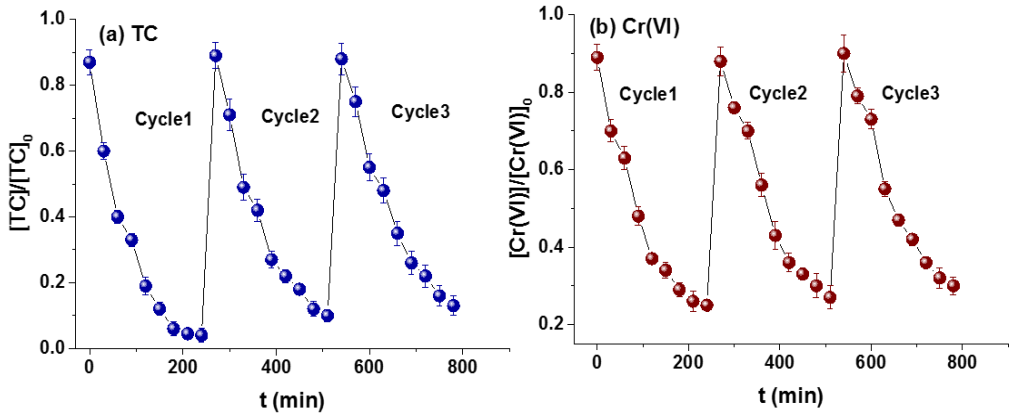

Figure 9. Reusability experiments for photocatalytic decontamination of TC and Cr(VI) in the *M. aeruginosa*-PAN/TiO_2/Ag NF system.

3. Materials and Methods

3.1. Materials

Polyacrylonitrile (PAN, Mw = 150 k) was obtained from Aldrich. Anatase particles (TiO_2, sized 5–10 nm) were obtained from Evonik Industries Metal Oxides (Beijing, China). Electrospinning solvent DMF, $K_2Cr_2O_7$, and $AgNO_3$ were provided by Beijing Chemical Works (Beijing, China). Tetracycline hydrochloride (TC), potassium iodide (KI), 2-propanol, 1,4-benzoquinone (BQ), and carbon tetrachloride (CCl_4) were purchased from Aladdin (Shanghai, China). Methanol and formic acid (FA) were HPLC grade and obtained from Fisher Chemical (Beijing, China). *M. aeruginosa* was obtained from Wuhan Hydrobiology Institute of CAS, China. Milli-Q water was used to prepare all the aqueous solutions (Millipore Corp, Boston, MA, USA). All the other chemicals were analytical grade and were further used without purification.

3.2. Preparation of M. aeruginosa-Decorated PAN/TiO2/Ag Nanofiber Mats

A quantity of 10 wt% of electrospinning solution was obtained by stirring the PAN in DMF mixture at 50 °C for 24 h. A certain amount of $AgNO_3$ and TiO_2 was dispersed in the above mixture by ultrasonic treatment. Subsequently, the spinning solution was put into a glass syringe and connected to a high-voltage power supply (Spellman SL150, New York, NY, USA). Electrospinning was performed at 10 kV with constant collection distance of 15 cm. A syringe pump was used to feed the polymer solution at a rate of 0.25 mL h^{-1}. A schematic diagram of the single needle electrospinning setup is presented in Figure 1a. Nanofibers were collected on the aluminum foil and dried under vacuum and room temperature for 24 h.

M. aeruginosa-decorated PAN/TiO_2/Ag NF were prepared by placing 5 mL of *M. aeruginosa* solution (1.0×10^9 cells L^{-1}) on the PAN/TiO_2/Ag NF (0.5 g, 5 × 5 cm) and incubated for 72 h to let adequate attachment of the microalgae to nanofibers (Figure 10b). All of the samples were washed at least three times with pure water to remove residues and unstable algae cells. The interaction between algae and PAN/TiO_2/Ag NF was analyzed by the UV-vis spectrum [33,34].

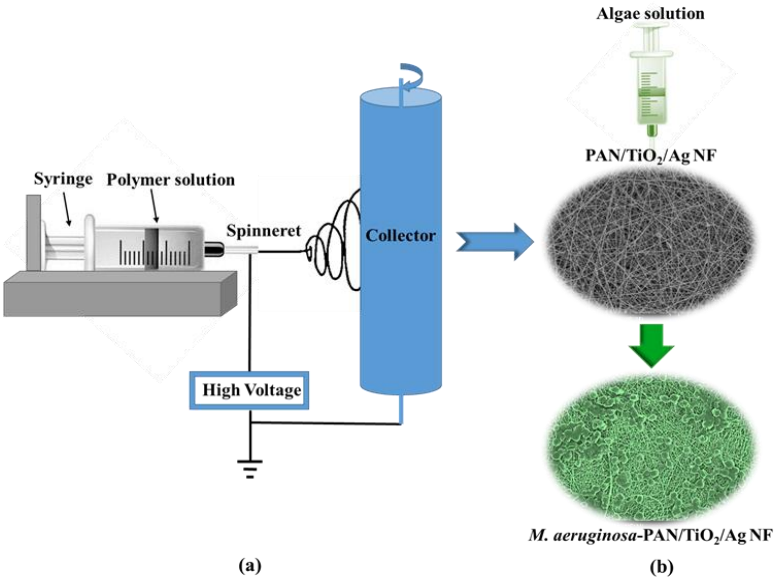

Figure 10. (**a**) Schematic diagram of electrospinning setup and (**b**) diagram illustrating the preparation of *M. aeruginosa*-TiO_2/Ag hybrid nanofiber.

3.3. Characterizations of M. aeruginosa-Decorated PAN/TiO2/Ag Nanofiber Mats

The synthesized nanofibers were characterized by transmission electron microscopy (TEM, Tecnai G2 20 ST, Hillsboro, CA, USA) and scanning electron microscopy (SEM, Jeol Co., Akishima, Japan). Elemental composition of nanofibers was also investigated by energy dispersive X-ray

spectroscopy (EDX, Horiba, Kyoto, Japan). The BET specific surface area of the nanofiber was characterized by the surface area and porosity of the analyzer (ASAP 2020 HD88, Micromeritics, Norcross, GA, USA). The UV–vis spectra of hybrid nanofiber mats were characterized by a UV–vis Spectrophotometer (Shimadzu UV-3101, Kyoto, Japan).

3.4. Photocatalytic Activity Measurement

The photocatalytic activity of *M. aeruginosa* decorated PAN/TiO_2/Ag NF was measured by the decontamination of TC and Cr(VI) under visible-light irradiation. Photocatalytic degradation studies were conducted using a homemade photochemical reactor (1 L) connected with 500 W halogen lamp (made by Institute of Electric Light Source of Beijing, China) and an optical filter to cut off the UV wave-length (λ < 420 nm). All the reaction solutions were prepared by adding the prepared *M. aeruginosa*-PAN/TiO_2/Ag NF into 500 mL aqueous solutions containing TC (20 mg L^{-1}) and Cr(VI) (10 mg L^{-1}). Systems with only PAN/TiO_2/Ag NF and *M. aeruginosa* were set as controls. Five mL of *M. aeruginosa* solution (1.0×10^9 cells L^{-1}) were diluted into a 500 mL reaction solution, and the total algae amount was equal to the immobilized cells on the nanofibers; the PAN/TiO_2/Ag NF (1 g L^{-1}) was the same amount as that used for algae immobilization. The pH of the reaction solution was kept at 6.0. Before the irradiation experiment, the mixture was kept in dark and ambient conditions for 30 min to achieve the adsorption-desorption equilibrium. During the photoreaction process, 5 mL of sample was collected at pre-set time intervals, and all the samples were filtered using a 0.25 μm membrane. The TC concentration was determined by HPLC (Agilent 1200, PaloAlto, CA, USA) with a Waters C18 column (3.5 μm, 4.6 × 150 mm) and UV detection at 355 nm. The volume ratio of 0.2% of FA water and methanol was 5:5 (*v*/*v*) with a flow rate of 0.5 mL min^{-1}. The Cr(VI) concentration was determined through spectrophotometric assay in the presence of diphenylcarbazide as coloring agent (Shimadzu UV-3101 Spectrometer, Kyoto, Japan). Moreover, all of the experiments were conducted in triplicate.

To investigate the photocatalytic mechanism of the *M. aeruginosa*-decorated PAN/TiO_2/Ag NF, experiments were performed using 1 mM of various scavengers. For example, CCl_4 [35,36], 2-propanol [37], KI [38], and BQ [39,40] served as scavengers to trap the electrons, hydroxyl radicals (·OH), holes, and superoxide radical ($O_2^{\cdot-}$), respectively. However, all other experimental conditions were the same as in the photodegradation experiment.

3.5. Photodegradation of Algae

After irradiation for 4 h, the MDA and SOD of the algae were determined using a reagent kit (Nanjing Jiancheng Biotechnology Institute, Nanjing, China) [41,42]. Microcystins were detected in the system using an ELISA kit for total-microcystins detection (J&Q Environmental Technologies Co., Ltd., Hong Kong, China).

4. Conclusions

We have reported the successful preparation of *M. aeruginosa*-decorated PAN/TiO_2/Ag NF to synergistically enhance the photocatalytic activity for the removal of organic (TC) and inorganic (Cr(VI)) pollutants under visible light irradiation. The reaction rate constants (*k*) of TC and Cr(VI) degradation by *M. aeruginosa*-PAN/TiO_2/Ag NF were 2.4 and 1.5-folder higher than that of bare PAN/TiO_2/Ag NF. Algae cells not only improved the absorption ability of pollutants but also accelerated the photodegradation of toxic pollutants. This study can help explain one of the possible transformation pathways of pollutants in the aquatic ecosystem, such as in lakes and rivers. Irradiation in the presence of PAN/TiO_2/Ag NF caused damage to algae cells, but microcystin was not detected in the solution, indicating the simultaneous photodegradation of microcystin in the system. This study is novel, as it converts harmful algae into useful photoreactive bionano hybrid materials for removing other pollutants. Bionano hybrid materials can be reused and easily removed from the solution after the reaction, providing a promising and sustainable strategy to remove toxic pollutants from effluents under visible light irradiation.

Supplementary Materials: The following are available online at www.mdpi.com/xxx/s1: Figure S1: UV-vis absorption spectra of the washing solutions, Figure S2: Variation of UV–vis absorption spectra of algae supernatant after irradiation.

Author Contributions: L.W. and C.Z. designed the experiments and prepared the original draft. R.C. contributed with SEM and TEM characterization. J.A. contributed with photocatalytic experiments. Z.W., G.M., and G.P. wrote and commented on the manuscript. All authors discussed the experimental results and edited the manuscript.

Funding: This work was founded by the National Key R&D Program of China (2017YFA0207203), Science and Technology Service Network Initiative (KFJ-STS-ZDTP-048), the Key Research and Development Program of Ningxia (2017BY064), Science and Technology Innovation Project from the Chinese Academy of Agricultural Sciences (CAAS-XTCX2016018), National Natural Science Foundation of China (21407160, 21107055), Natural Science Funds Fund from Tianjin (13JCYBJC20300) and Strategic Priority Research Program of the Chinese Academy of Sciences (XDA09030203).

Acknowledgments: Thank C.Z. and R.C. for the careful revision of this article. Especially wants to thank the great support from Z.W. and G.P. during the research.

Conflicts of Interest: The authors declare no conflict of interest.

References

1. Ali, J.; Sohail, A.; Wang, L.; Haider, M.R.; Mulk, S.; Pan, G. Electro-microbiology as a promising approach towards renewable energy and environmental sustainability. *Energies* **2018**, *11*, 1–30, doi:10.3390/en11071822.
2. Deng, L.; Wang, H.; Deng, N. Photoreduction of chromium(VI) in the presence of algae, Chlorella vulgaris. *J. Hazard. Mater.* **2006**, *138*, 288–292, doi:10.1016/j.jhazmat.2006.04.062.
3. Deng, L.; Wu, F.; Deng, N.; Zuo, Y. Photoreduction of mercury(II) in the presence of algae, Anabaena cylindrical. *J. Photochem. Photobiol. B* **2008**, *91*, 117–124, doi:10.1016/j.jphotobiol.2008.02.005.
4. Liu, X.L.; Wu, F.; Deng, N. Photoproduction of hydroxyl radicals in aqueous solution with algae under high-pressure mercury lamp. *Environ. Sci. Technol.* **2004**, *38*, 296–299, doi:10.1021/es034626b.
5. Zepp, R.G.; Schlotzhauer, P.F. Influence of algae on photolysis rates of chemicals in water. *Environ. Sci. Technol.* **1983**, *17*, 462–468, doi:10.1021/es00114a005.
6. Peng, Z.e.; Wu, F.; Deng, N. Photodegradation of bisphenol A in simulated lake water containing algae, humic acid and ferric ions. *Environ. Pollut.* **2006**, *144*, 840–846, doi:10.1016/j.envpol.2006.02.006.
7. Zhang, J.W.; Ma, L. Photodegradation mechanism of sulfadiazine catalyzed by Fe(III), oxalate and algae under UV irradiation. *Environ. Technol.* **2013**, *34*, 1617–1623, doi:10.1080/09593330.2013.765915.
8. Li, H.; Pan, G. Simultaneous removal of harmful algal blooms and microcystins using microorganism- and chitosan-modified local soil. *Environ. Sci. Technol.* **2015**, *49*, 6249–6256, doi:10.1021/acs.est.5b00840.
9. Pan, G.; Dai, L.; Li, L.; He, L.; Li, H.; Bi, L.; Gulati, R.D. Reducing the recruitment of sedimented algae and nutrient release into the overlying water using modified soil/sand flocculation-capping in eutrophic lakes. *Environ. Sci. Technol.* **2012**, *46*, 5077–5084, doi:10.1021/es3000307.
10. Eroglu, E.; Agarwal, V.; Bradshaw, M.; Chen, X.; Smith, S.M.; Raston, C.L.; Iyer, K.S. Nitrate removal from liquid effluents using microalgae immobilized on chitosan nanofiber mats. *Green Chem.* **2012**, *14*, 2682–2685, doi:10.1039/c2gc35970g.
11. Nalbandian, M.J.; Zhang, M.L.; Sanchez, J.; Kim, S.; Choa, Y.H.; Cwiertny, D.M.; Myung, N.V. Synthesis and optimization of Ag-TiO_2 composite nanofibers for photocatalytic treatment of impaired water sources. *J. Hazard. Mater.* **2015**, *299*, 141–148, doi:10.1016/j.jhazmat.2015.05.053.
12. Amarjargal, A.; Tijing, L.D.; Ruelo, M.T.G.; Lee, D.H.; Kim, C.S. Facile synthesis and immobilization of Ag-TiO_2 nanoparticles on electrospun PU nanofibers by polyol technique and simple immersion. *Mater. Chem. Phys.* **2012**, *135*, 277–281, doi:10.1016/j.matchemphys.2012.05.078.
13. Pant, H.R.; Pandeya, D.R.; Nam, K.T.; Baek, W.I.; Hong, S.T.; Kim, H.Y. Photocatalytic and antibacterial properties of a TiO_2/nylon-6 electrospun nanocomposite mat containing silver nanoparticles. *J. Hazard. Mater.* **2011**, *189*, 465–471, doi:10.1016/j.jhazmat.2011.02.062.
14. Veres, A.; Rica, T.; Janovak, L.; Domok, M.; Buzas, N.; Zollmer, V.; Seemann, T.; Richardt, A.; Dekany, I. Silver and gold modified plasmonic TiO_2 hybrid films for photocatalytic decomposition of ethanol under visible light. *Catal. Today* **2012**, *181*, 156–162, doi:10.1016/j.cattod.2011.05.028.

15. Rana, S.; Nazar, U.; Ali, J.; Ali, Q.u.A.; Ahmad, N.M.; Sarwar, F.; Waseem, H.; Jamil, S.U.U. Improved antifouling potential of polyether sulfone polymeric membrane containing silver nanoparticles: Self-cleaning membranes. *Environ. Technol.* **2018**, *39*, 1413–1421.
16. Chang, J.; Wang, J.; Qu, J.; Li, Y.V.; Ma, L.; Wang, L.; Wang, X.; Pan, K. Preparation of alpha-Fe_2O_3/polyacrylonitrile nanofiber mat as an effective lead adsorbent. *Environ. Sci. Nano* **2016**, *3*, 894–901, doi:10.1039/c6en00088f.
17. Morillo, D.; Faccini, M.; Amantia, D.; Perez, G.; Garcia, M.A.; Valiente, M.; Aubouy, L. Superparamagnetic iron oxide nanoparticle-loaded polyacrylonitrile nanofibers with enhanced arsenate removal performance. *Environ. Sci. Nano* **2016**, *3*, 1165–1173, doi:10.1039/c6en00167j.
18. Abdolmaleki, A.; Mallakpour, S.; Borandeh, S. In situ synthesis of silver nanoparticles in novel L-phenylalanine based poly(amide-benzimidazole-imide) matrix through metal complexation method using *N,N′*-dimethylformamide as a reaction medium and reducing agent. *Polym. Plast. Technol. Eng.* **2015**, *54*, 1002–1008, doi:10.1080/03602559.2014.974276.
19. Wang, T.Y.; Quan, W.; Jiang, D.L.; Chen, L.L.; Li, D.; Meng, S.; Chen, M. Synthesis of redox-mediator-free direct Z-scheme AgI/WO_3 nanocomposite photocatalysts for the degradation of tetracycline with enhanced photocatalytic activity. *Chem. Eng. J.* **2016**, *300*, 280–290, doi:10.1016/j.cej.2016.04.128.
20. Wang, H.W.; Zhang, D.Y.; Mou, S.; Song, W.; Al-Misned, F.A.; Mortuza, M.G.; Pan, X.L. Simultaneous removal of tetracycline hydrochloride and As(III) using poorly-crystalline manganese dioxide. *Chemosphere* **2015**, *136*, 102–110, doi:10.1016/j.chemosphere.2015.04.070.
21. Chen, Y.; Liu, K.R. Preparation and characterization of nitrogen-doped TiO_2/diatomite integrated photocatalytic pellet for the adsorption-degradation of tetracycline hydrochloride using visible light. *Chem. Eng. J.* **2016**, *302*, 682–696, doi:10.1016/j.cej.2016.05.108.
22. Xu, S.C.; Pan, S.S.; Xu, Y.; Luo, Y.Y.; Zhang, Y.X.; Li, G.H. Efficient removal of Cr(VI) from wastewater under sunlight by Fe(II)-doped TiO_2 spherical shell. *J. Hazard. Mater.* **2015**, *283*, 7–13, doi:10.1016/j.jhazmat.2014.08.071.
23. Qiu, R.; Zhang, D.; Diao, Z.; Huang, X.; He, C.; Morel, J.L.; Xiong, Y. Visible light induced photocatalytic reduction of Cr(VI) over polymer-sensitized TiO_2 and its synergism with phenol oxidation. *Water Res.* **2012**, *46*, 2299–2306, doi:10.1016/j.watres.2012.01.046.
24. Ali, J.; Ali, N.; Jamil, S.U.U.; Waseem, H.; Khan, K.; Pan, G. Insight into eco-friendly fabrication of silver nanoparticles by Pseudomonas aeruginosa and its potential impacts. *J. Environ. Chem. Eng.* **2017**, *5*, 3266–3272.
25. Yu, J.G.; Xiong, J.F.; Cheng, B.; Liu, S.W. Fabrication and characterization of Ag-TiO_2 multiphase nanocomposite thin films with enhanced photocatalytic activity. *Appl. Catal. B Environ.* **2005**, *60*, 211–221, doi:10.1016/j.apcatb.2005.03.009.
26. Ali, J.; Hameed, A.; Ahmed, S.; Ali, M.I.; Zainab, S.; Ali, N. Role of catalytic protein and stabilising agents in the transformation of Ag ions to nanoparticles by Pseudomonas aeruginosa. *IET Nanobiotechnol.* **2016**, *10*, 295–300, doi:10.1049/iet-nbt.2015.0093.
27. Kim, K.D.; Han, D.N.; Lee, J.B.; Kim, H.T. Formation and characterization of Ag-deposited TiO_2 nanoparticles by chemical reduction method. *Scr. Mater.* **2006**, *54*, 143–146, doi:10.1016/j.scriptamat.2005.09.054.
28. Seery, M.K.; George, R.; Floris, P.; Pillai, S.C. Silver doped titanium dioxide nanomaterials for enhanced visible light photocatalysis. *J. Photoch. Photobio. A.* **2007**, *189*, 258–263, doi:10.1016/j.jphotochem.2007.02.010.
29. Wang, L.; Zhang, C.; Gao, F.; Mailhot, G.; Pan, G. Algae decorated TiO_2/Ag hybrid nanofiber membrane with enhanced photocatalytic activity for Cr(VI) removal under visible light. *Chem. Eng. J.* **2017**, *314*, 622–630, doi:10.1016/j.cej.2016.12.020.
30. Luo, L.; Lai, X.; Chen, B.; Lin, L.; Fang, L.; Tam, N.F.Y.; Luan, T. Chlorophyll catalyse the photo-transformation of carcinogenic benzo a pyrene in water. *Sci. Rep.* **2015**, *5*, doi:10.1038/srep12776.
31. Wang, K.; Garg, S.; Waite, T.D. Light-mediated reactive oxygen species generation and iron redox transformations in the presence of exudate from the cyanobacteriurn microcystis aeruginosa. *Environ. Sci. Technol.* **2017**, *51*, 8384–8395, doi:10.1021/acs.est.7b01441.
32. Wang, L.; Zhang, C.; Wu, F.; Deng, N. Photodegradation of aniline in aqueous suspensions of microalgae. *J. Photochem. Photobiol. B* **2007**, *87*, 49–57, doi:10.1016/j.jphotobiol.2006.12.006.

33. Vitiello, G.; Pezzella, A.; Zanfardino, A.; Varcamonti, M.; Silvestri, B.; Costantini, A.; Branda, F.; Luciani, G. Titania as a driving agent for DHICA polymerization: A novel strategy for the design of bioinspired antimicrobial nanomaterials. *J. Mater. Chem. B* **2015**, *3*, 2808–2815, doi:10.1039/c5tb00039d.
34. Vitiello, G.; Pezzella, A.; Calcagno, V.; Silvestri, B.; Raiola, L.; D'Errico, G.; Costantini, A.; Branda, F.; Luciani, G. 5,6-dihydroxyindole-2-carboxylic-acid-TiO_2 charge transfer complexes in the radical polymerization of melanogenic precursor(s). *J. Phys. Chem. C* **2016**, *120*, 6262–6268, doi:10.1021/acs.jpcc.6b00226.
35. Saeki, A.; Yamamoto, N.; Yoshida, Y.; Kozawa, T. Geminate charge recombination in liquid alkane with concentrated CCl_4: Effects of CCl_4 radical anion and narrowing of initial distribution of Cl. *J. Phys. Chem. A* **2011**, *115*, 10166–10173, doi:10.1021/jp205989r.
36. Qu, L.N.; Lang, J.Y.; Wang, S.W.; Chai, Z.L.; Su, Y.G.; Wang, X.J. Nanospherical composite of WO_3 wrapped $NaTaO_3$: Improved photodegradation of tetracycline under visible light irradiation. *Appl. Surf. Sci.* **2016**, *388*, 412–419, doi:10.1016/j.apsusc.2015.12.095.
37. Chen, Y.; Hu, C.; Hu, X.X.; Qu, J.H. Indirect photodegradation of amine drugs in aqueous solution under simulated sunlight. *Environ. Sci. Technol.* **2009**, *43*, 2760–2765, doi:10.1021/es803325j.
38. Cai, L.; Xiong, X.L.; Liang, N.G.; Long, Q.Y. Highly effective and stable Ag_3PO_4-WO_3/MWCNTs photocatalysts for simultaneous Cr(VI) reduction and orange II degradation under visible light irradiation. *Appl. Surf. Sci.* **2015**, *353*, 939–948, doi:10.1016/j.apsusc.2015.07.028.
39. Wang, S.; Li, D.; Sun, C.; Yang, S.; Guan, Y.; He, H. Synthesis and characterization of g-C_3N_4/Ag_3VO_4 composites with significantly enhanced visible-light photocatalytic activity for triphenylmethane dye degradation. *Appl. Catal. B Environ.* **2014**, *144*, 885–892, doi:10.1016/j.apcatb.2013.08.008.
40. Peng, B.; Zhang, S.; Yang, S.; Wang, H.; Yu, H.; Zhang, S.; Peng, F. Synthesis and characterization of g-C_3N_4/Cu_2O composite catalyst with enhanced photocatalytic activity under visible light irradiation. *Mater. Res. Bull.* **2014**, *56*, 19–24, doi:10.1016/j.materresbull.2014.04.042.
41. Deng, X.; Wu, F.; Liu, Z.; Luo, M.; Li, L.; Ni, Q.; Jiao, Z.; Wu, M.; Liu, Y. The splenic toxicity of water soluble multi-walled carbon nanotubes in mice. *Carbon* **2009**, *47*, 1421–1428, doi:10.1016/j.carbon.2008.12.032.
42. Rocchetta, I.; Mazzuca, M.; Conforti, V.; Ruiz, L.; Balzaretti, V.; de Molina, M.d.C.R. Effect of chromium on the fatty acid composition of two strains of Euglena gracilis. *Environ. Pollut.* **2006**, *141*, 353–358, doi:10.1016/j.envpol.2005.08.035.